An Arbitrary Lagrangian Eulerian Formulation for IsoGeometric Discontinuous Galerkin Schemes

Stefano Pezzano, Régis Duvigneau

Université Côte d'Azur, Inria, CNRS, LJAD
e-mail: stefano.pezzano@inria.fr, regis.duvigneau@inria.fr

IGA Conference, Munich, 18-20 September 2019

Outline

Outline

Key ideas

- Discontinuous Galerkin schemes combine advantages of Finite Volumes and Continuous Finite Elements:
  - local conservation
  - numerical stability via Riemann solver
  - high-order accuracy, low numerical dissipation
  - handling of arbitrary meshes
- IsoGeometric DG[1]: elements are rational Bezier patches extracted from NURBS geometry
- Goals of present work:
  - extending the IDG framework to time dependent geometries
  - quantify the gain of using high-order meshes

[1] R. Duvigneau, *Isogeometric analysis for compressible flows using a Discontinuous Galerkin method*, Comput. Methods Appl. Mech. Engrg. 333 (2018), 443-461

DG formulation

- Considering a system of conservation laws:

$$\frac{\partial \mathbf{W}}{\partial t} + \nabla \cdot \mathbf{F} = 0,$$

- In each element, discrete solution $\mathbf{w}_h$ represented as:

$$\mathbf{w}_h^e(\mathbf{x}, t) = \sum_i R_i^e(\mathbf{x})\mathbf{w}_i^e(t)$$

- R_i are rational Bernstein functions, w_i are the DOFs
- The weak formulation is:

$$\int_{\Omega_e} R_k^e \frac{\partial \mathbf{w}_h^e}{\partial t} d\Omega = \int_{\Omega_e} \nabla R_k^e \cdot \mathbf{F}(\mathbf{w}_h^e) d\Omega - \oint_{\partial\Omega_e} R_k^e \mathbf{F}^* d\Gamma$$

DG formulation, cont'd

- Elements coupled through numerical flux $\mathbf{F}^*$
- $\mathbf{F}^* = \mathbf{F}^*(\mathbf{w}_h^+, \mathbf{w}_h^-, \mathbf{n})$ is a consistent Riemann solver:

$$\mathbf{F}^*(\mathbf{w}_0, \mathbf{w}_0, \mathbf{n}) = \mathbf{F}(\mathbf{w}_0) \cdot \mathbf{n}$$

- Space integrals computed through Gauss quadrature
- Time evolution of DOFs described by system of ODEs:

$$\mathcal{M}\frac{d\mathbf{w}}{dt} = \mathcal{R}(\mathbf{w}_h)$$

- Explicit Runge-Kutta (RK4 or RK3 SSP) method for time integration

ALE scheme

- The formulation proposed by Nguyen[2] is adopted:

$$\frac{d}{dt}\int_{\Omega_e} R_k \mathbf{w}_h d\Omega = \int_{\Omega_e} \nabla R_k \cdot \left[\mathbf{F}(\mathbf{w}_h) - \mathbf{V}_g \mathbf{w}_h\right] d\Omega - \oint_{\partial\Omega_e} R_k \mathbf{F}^*_{ale} d\Gamma$$

- Consistency condition for $\mathbf{F}^*_{ale} = \mathbf{F}^*_{ale}(w_h^+, w_h^-, \mathbf{V}_g, \mathbf{n})$ becomes:

$$\mathbf{F}^*_{ale}(\mathbf{w}_0, \mathbf{w}_0, \mathbf{V}_g, \mathbf{n}) = \mathbf{F}(\mathbf{w}_0) \cdot \mathbf{n} - (\mathbf{V}_g \cdot \mathbf{n})\mathbf{w}_0$$

- Constant solutions preserved when Gauss quadrature is exact
- Mass matrix is time dependent:

$$\frac{d}{dt}(\mathcal{M}\mathbf{w}) = \mathcal{R}(\mathbf{w}_h, \mathbf{V}_g)$$

[2] V. T. Nguyen, *An arbitrary Lagrangian-Eulerian discontinuous Galerkin method for simulations of flows over variable geometries*, Journal of Fluids and Structures 26 (2010), 312-329

NURBS-based mesh movement

- Isoparametric paradigm used to define grid velocity field:

$$\mathbf{V}_g = \sum_{i=0}^{n} R_{i,n} \mathbf{V}_{g,i}$$

- Time evolution of control point net:

$$\frac{d\mathbf{X}_i}{dt} = \mathbf{V}_{g,i}$$

- Arbitrarily high-order deformations
- Explicit movement: distribution of $\mathbf{V}_{g,i}$ is imposed at each time step
- Integration with RK4 or RK3 SSP
- Possibility of using refined meshes with non-conformities

Outline

Isentropic vortex test case

- Euler equations
- Advection of an isentropic vortex:

$$\begin{cases} \rho = \left(1 - \frac{\gamma-1}{16\gamma\pi^2}\beta^2 e^{2(1-r^2)}\right)^{\frac{1}{\gamma-1}} \\ u = 1 - \beta e^{1-r^2}\frac{y-y_0}{2\pi} \\ v = \beta e^{1-r^2}\frac{x-t-x_0}{2\pi} \\ p = \rho^\gamma \end{cases}$$

- Two configurations are compared:
  - fixed mesh
  - deforming mesh: $u_g(\mathbf{x}, t) = v_g(\mathbf{x}, t) = \sin\left(\frac{\pi}{2}x\right)\sin\left(\frac{\pi}{2}y\right)\sin(2\pi t)$

Error analysis

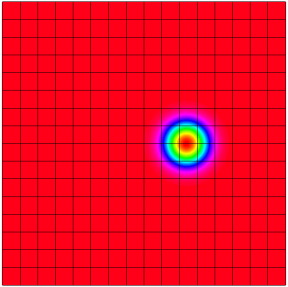

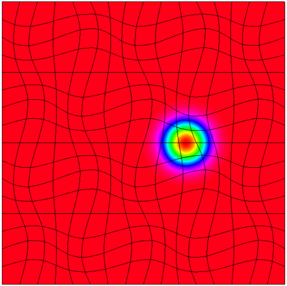

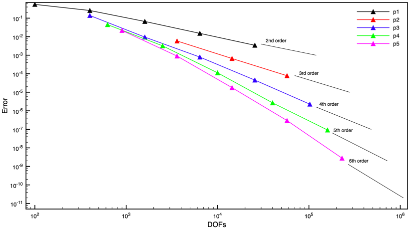

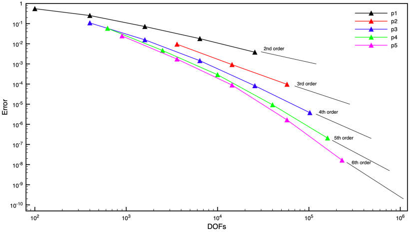

Outline

Numerical setup

Viscous flow around a vertically oscillating cylinder. Setup:

- Mach number: 0.2
- Reynolds number: 500
- Oscillation amplitude: 0.25D
- Oscillation frequency: $0.875F_{sh}$
- Exact cylinder representation, using rational functions
- Polynomial degree: 3, 4, 5
- 3 mesh refinement levels, with 1065, 2145 and 4455 elements

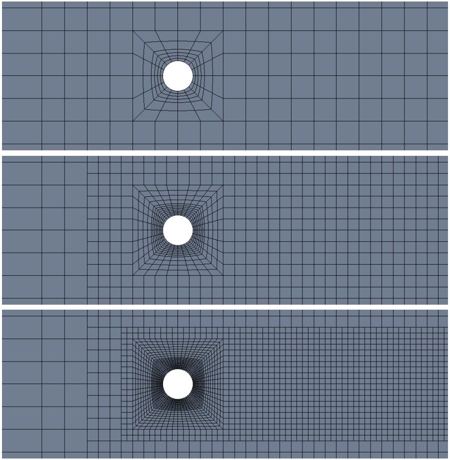

Figure: mesh levels

The lock-in phenomenon

- Vortex shedding synchronized with cylinder oscillation.
- Test case very sensitive to far-field boundary position.
- Good agreement with numerical results available in literature.[3]

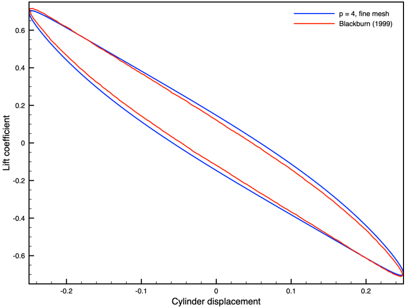

Figure: result comparison

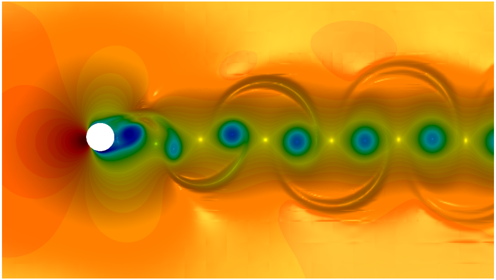

Figure: density, $p = 4$, fine mesh

[3] H. M. Blackburn, R. D. Henderson, *A study of two-dimensional flow past an oscillating cylinder*, J. Fluid Mech. 385 (1999), 255-286

Mesh convergence

- Lock-in well reproduced with all the polynomial degrees.
- Using high order basis functions on very coarse meshes does not improve significantly the results.
- Faster convergence with degree 4 and 5.
- Higher order basis affected by severe stability restrictions.
- Optimal degree and refinement depend on required accuracy.

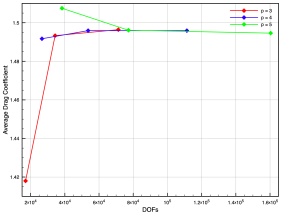

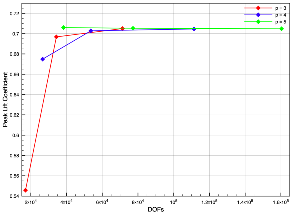

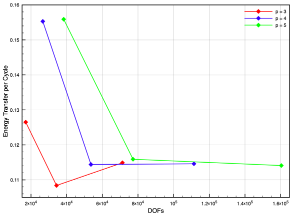

Mesh movement test

- Two movement laws:
  - rigid oscillation,
  - smooth deformation with Gaussian decay.
- Freestream well preserved, even with rational functions.
- Nearly identical results.

	rigid	smooth
$\hat{C}_L$	0.7046	0.7046
$\bar{C}_D$	1.4959	1.4945
E	0.1146	0.1148

Table: p = 4, fine mesh

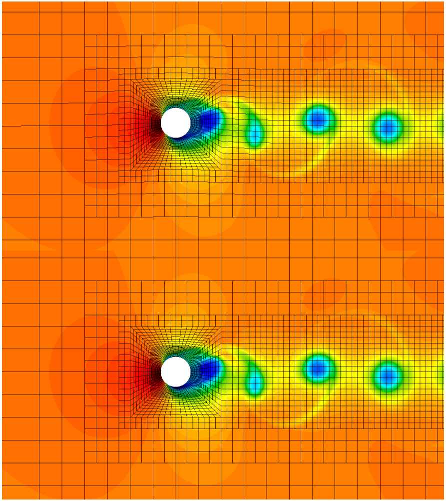

Figure: density, p = 4, fine mesh

Outline

Test case configuration

Compressible flow around a pitching NACA 0012 airfoil:

- cubic polynomial basis
- 4 mesh refinement levels: 700, 1720, 4092 and 11272 elements
- comparison with corresponding linear mesh
- pitch amplitude:
  - Euler: 5°
  - Navier-Stokes: 20°
- reduced frequency: 0.25
- Mach number: 0.2
- Reynolds number (NS): 1000

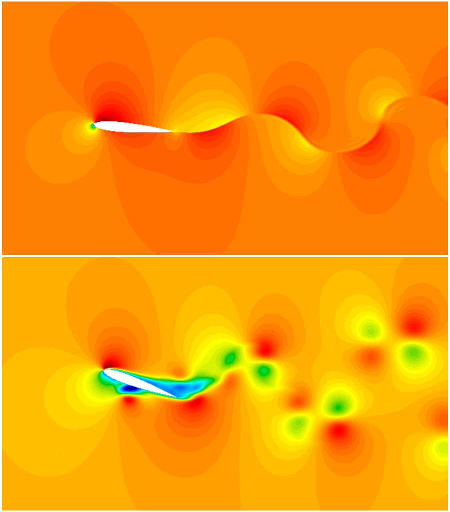

Figure: streamwise momentum, inviscid (top) and viscous (bottom)

Influence of the geometry: inviscid flow

- Benefits of curve mesh clearly visible.
- Spurious expansion fans develops at element vertices on linear meshes.
- Flow-tangency boundary conditions depends on the normal, which is piecewise constant.

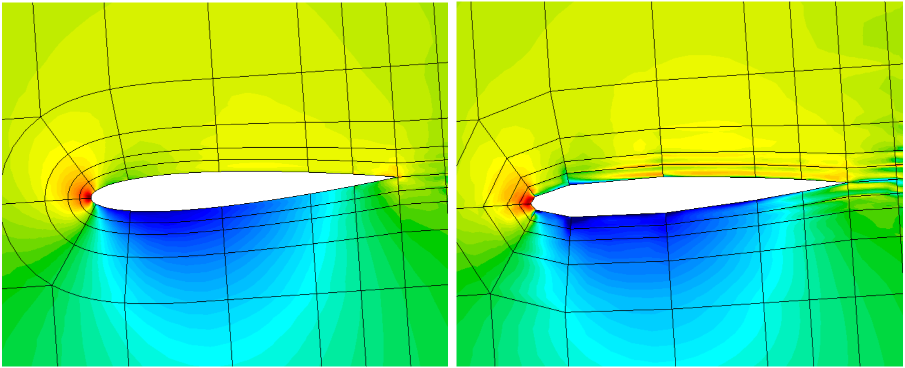

Figure: 700 elements mesh, density

Influence of the geometry: viscous flow

- Similar results, even on very coarse meshes.
- No-slip boundary conditions depends on the position, which is piecewise linear.
- Viscosity has a regularizing effect.

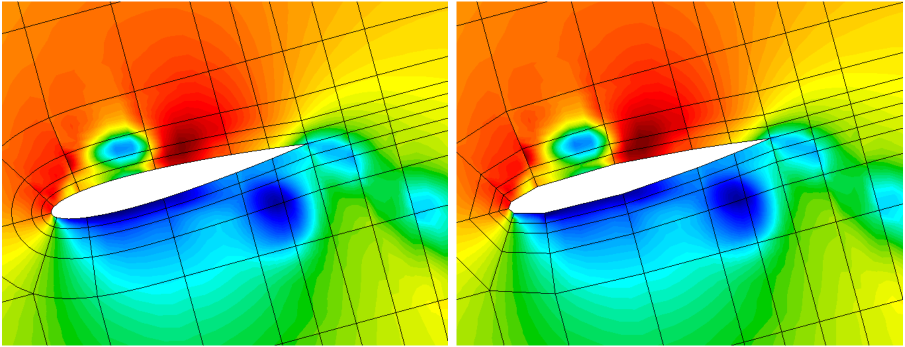

Figure: 700 elements mesh, density

Influence of the geometry: mesh convergence

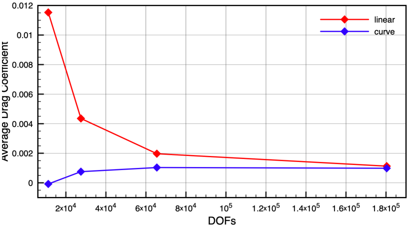

Figure: Inviscid flow, $\bar{C}_D$

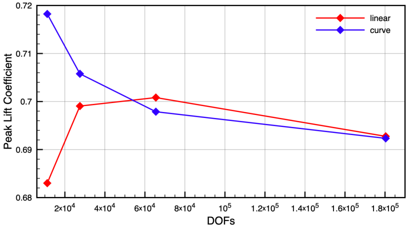

Figure: Inviscid flow, $\hat{C}_L$

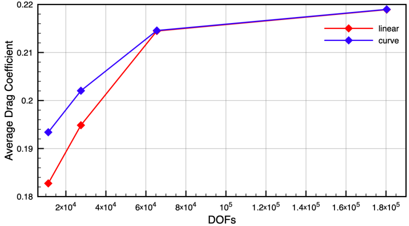

Figure: Laminar flow, $\bar{C}_D$

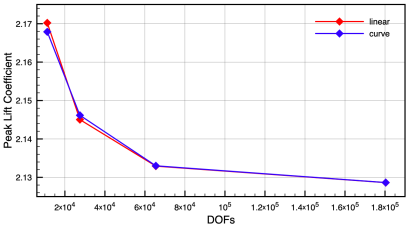

Figure: Laminar flow, $\hat{C}_L$

Conclusions and perspectives

- IsoGeometric DG successfully extended to time dependent geometries:
    - arbitrarily high-order deformation fields on non-conformal grids
    - optimal convergence rates for compressible flow problems
    - mesh deformation does not impact accuracy of the scheme
    - use of rational elements in ALE formulation
- Gain of using high-order geometry is problem dependent
- Further developments:
    - sliding meshes
    - ALE with dynamic grid adaptation

Thanks for your attention!